Structural Studies of Commensurate Peierls State of $Rb_{1.67}[Pt(C_2O_4)_2]\cdot 1.5H_2O$

Akiko KOBAYASHI,* Yukiyoshi SASAKI, and Hayao KOBAYASHI**

Department of Chemistry, The Research Centre for Spectrochemistry, Faculty of Science, The University of Tokyo, Hongo, Tokyo 113

***Department of Chemistry, Faculty of Science, Toho University, Funabashi, Chiba 274*

(Received May 17, 1979)

X-Ray examination, chemical analyses and electrical conductivity measurements have been conducted on the partially oxidized platinum complex $Rb_{1.67}[Pt(C_2O_4)_2]\cdot 1.5H_2O$ (RbDOX). The cell constants are $a=12.690(10)$, $b=17.108(14)$, $c=11.357(3)$ Å; $\alpha=102.04(4)$, $\beta=115.17(3)$, $\gamma=43.58(4)°$, and the space group is $P\bar{1}$. The planar bis(oxalato)platinate ions stack along the crystallographic b axis and the Pt atoms form a sixfold distorted chain. RbDOX is the first example of a sixfold structure. Three independent Pt–Pt distances are 2.717(3), 2.830(3), and 3.015(3) Å. The Pt–Pt distance of 2.717 Å is the shortest spacing so far observed in partially oxidized platinate salts and shorter than the 2.77 Å interatomic separation in Pt metal itself. The oxalate ligands are staggered (46°, 55°, 80°) with respect to the ligands directly above and below them along the chain. Sixfold modulated superstructure of RbDOX is confirmed as the newly found commensurate Peierls structure based on agreement with the period of the Peierls distorted superlattice determined by the degree of partial oxidation. The calculation of Coulomb energy shows that RbDOX has a crystal lattice in which the interchain Coulomb energies are at a minimum indicating the strong tendency of the anti-phase ordering of the nearest-neighbour Pt chains.

In recent years there has been considerable interest in the partially oxidized quasi-one-dimensional cyanoplatinates and bis(oxalato)platinates because of their high, newly metallic electrical conductivities and they provide experimental results which greatly aid the development of the theory of the one-dimensional state. The prototype compounds of cyanoplatinates groups are the anion deficient derivatives, $K_2[Pt(CN)]_4Br_{0.3}\cdot 3.2H_2O$ referred to as KCP. Since the original discovery by Comès *et al.*[1] of X-ray diffuse scattering associated with the Peierls instability in KCP, the nature of the sinusoidal modulation of one-dimensional platinum chain has been studied by many authors.[2,3]

In one-dimensional metals, modulation waves (charge density waves: CDWs) have a wave vector $q=2k_F$ in the chain direction, where k_F is the Fermi wave vector, and in the insulating state, the CDWs are correlated to form a three-dimensional static Peierls distortion, that is, the lattice modulation waves give rise to a three-dimensional superstructure at low temperature.[4] The period of the lattice modulation wave in the Peierls phase is commensurate or incommensurate with the period in the high-temperature metallic phase.

There has been much research on KCP salts and TTF-TCNQ (tetrathiafulvalene-7,7,8,8-tetracyanoquinodimethane),[5] however, the crystal structure determination of the Peierls state of the one-dimensional conductors appears to be very limited. The modulated superstructure of $K_{1.81}[Pt(C_2O_4)_2]\cdot 2H_2O$ (γ-KDOX)[6,7] is the first example of the incommensurate Peierls state determined by X-ray analysis and it is attributed to the condensation of the $2k_F$ phonon of the one-dimensional metallic system. In the present work the sixfold modulated commensurate Peierls structure of a new salt $Rb_{1.67}[Pt(C_2O_4)_2]\cdot 1.5H_2O$ (RbDOX) will be reported.

Experimental

RbDOX was prepared from $Rb_2[Pt(C_2O_4)_2]$ and Rb_2PtCl_6 by a diffusion method. The solution was allowed to stand for a month and copper-colored needle-shaped crystals deposited. Many of the crystals were twinned, the twin axis being the needle axis. A suitable untwinned specimen was selected for data collection. The crystal needle axis was chosen as the axis for mounting and the crystallographic b axis. Oscillation photographs showed reciprocal lattice layers for which $k=6n$ were especially strong and all others were very weak. This feature clearly indicates the existence of a Pt chain with Pt atoms stacked $b/6$ apart.

Collection and Reduction of the Data. The crystal selected for data collection had dimensions of $0.28\times 0.10\times 0.038$ mm. The data were collected on a Rigaku automated diffractometer equipped with a graphite monochromator. A least-squares fit of the diffractometer angles obtained by automatically centering reflections in the range $30°<2\theta<40°$ (Mo $K\alpha$ radiation, $\lambda=0.71069$ Å) yielded the following crystal data: $a=12.690$ (10), $b=17.108$ (14), $c=11.357$ (3) Å, $\alpha=102.04$ (4), $\beta=115.17$ (3), $\gamma=43.58$ (4)°, $V=1518.6$ Å^3, $Z=6$, $d_{calcd}=3.549$ g cm^{-3}, μ(Mo $K\alpha$)$=230.6$ cm^{-1}.

Intensity data were collected with monochromatized Mo $K\alpha$ radiation by the ω-2θ scan technique up to $2\theta=60°$. Reflections were scanned at the rate of 4° per minute in 2θ. Background counts of 10s were taken at each end of the scan range. The diffracted intensity gradually decreased to 93% of the initial value during X-ray radiation. The data were corrected for deterioration, but no corrections were made for absorption owing to the irregularity of the crystal shape.

Solution and Refinement of the Structure. The structure was solved using a Patterson map. Space group $P\bar{1}$ was provisionally chosen and Pt(1) and Pt(4) were assigned to special positions at (0, 0, 0) and (0, 1/2, 0), while Pt(2) and Pt(3) were initially placed at general positions. The atomic parameters were refined by the block-diagonal least-squares method, using anisotropic temperature factors for Pt and Rb atoms and isotropic factors for O and C atoms. The final R values are $R_1=0.069$ for $F_o>3\sigma(F_o)$ and $R_2=0.084$. The agreement indices are defined as $R_1=\sum w||F_o|-|F_o||/\sum w|F_o|$, $R_2=\sum w||F_o|^2-|F_c|^2|/\sum w|F_o|^2$. The weighting schemes used were: $w=1/[a+b|F_o|+c|F_o|^2]$ for $|F_o|\geq 45.64$ (absolute scale), $a=91.28$, $b=1.0$, and $c=0.00289$; $w=0.1$ otherwise. As the exact Rb ion composition and those of the water molecules are uncertain, the multipliers were varied in one of the final refinements with the full matrix least-squares method. The multipliers converged to approximately 1.0 for

Rb ions indicating that the Rb ion sites are fully occupied. The exact H_2O content could not be determined from the X-ray crystal structure refinement. The ambiguity in the H_2O composition may be related to the deterioration of the crystal. Large R values and abnormal bond lengths and angles were obtained by the noncentrosymmetric refinement in Pl and thus $P\bar{1}$ was confirmed as the correct space group.

Positional and thermal parameters determined from the final least-squares cycle are presented in Tables 1 and 2. The atomic scattering factors and the values of $\Delta f'$, $\Delta f''$, were taken from International Tables for X-Ray Crystallography.[8] The F_o-F_c Tables are kept at the office of this

Table 1. Fractional coordinates ($\times 10000$)

Atom	x	y	z	Atom	x	y	z
Pt (1)	0	0	0	C (6)	−3278 (32)	4738 (21)	−1215 (25)
Pt (4)	0	5000	0	O (11)	−3460 (23)	4580 (15)	−3445 (18)
Pt (2)	21 (1)	1581 (1)	33 (1)	O (12)	−4777 (25)	5368 (17)	−1564 (20)
Pt (3)	172 (1)	3166 (1)	132 (1)	O (13)	2056 (23)	712 (16)	1692 (19)
Rb (1)	2670 (4)	−697 (3)	−4627 (3)	O (14)	−1257 (24)	2470 (16)	1203 (19)
Rb (2)	4616 (4)	4011 (3)	−1270 (3)	C (7)	1623 (42)	1117 (28)	2734 (34)
Rb (3)	7128 (4)	3361 (2)	4238 (3)	C (8)	−140 (45)	2180 (30)	2429 (36)
Rb (4)	8651 (5)	−3216 (4)	−4986 (3)	O (15)	2759 (38)	583 (26)	3859 (30)
Rb (5)	5134 (4)	−1174 (3)	881 (3)	O (16)	−712 (41)	2837 (28)	3254 (33)
O (1)	−441 (23)	−29 (15)	−1948 (18)	O (17)	1241 (21)	784 (14)	−1170 (17)
O (2)	2367 (22)	−1235 (15)	282 (17)	O (18)	−2075 (20)	2454 (13)	−1634 (16)
C (1)	968 (32)	−851 (21)	−2098 (26)	C (9)	−1 (36)	1310 (24)	−2495 (29)
C (2)	2634 (31)	−1537 (20)	−852 (25)	C (10)	−1769 (29)	2132 (19)	−2679 (23)
O (3)	1044 (27)	−1060 (18)	−3209 (21)	O (19)	511 (27)	1080 (18)	−3329 (21)
O (4)	4012 (25)	−2240 (17)	−809 (20)	O (20)	−2826 (24)	2444 (16)	−3785 (20)
O (5)	2527 (22)	1918 (15)	311 (17)	O (21)	−1477 (25)	5498 (17)	−1963 (20)
O (6)	1325 (24)	2872 (16)	2106 (19)	O (22)	1888 (23)	3964 (15)	−574 (18)
C (3)	3681 (32)	1507 (21)	1494 (25)	C (11)	−501 (37)	5060 (25)	−2617 (30)
C (4)	2902 (30)	2111 (20)	2560 (24)	C (12)	1373 (34)	4203 (22)	−1827 (27)
O (7)	5139 (28)	725 (19)	1852 (23)	O (23)	−1160 (29)	5225 (19)	−3849 (23)
O (8)	3846 (26)	1887 (17)	3756 (21)	O (24)	2331 (31)	3798 (21)	−2363 (25)
O (9)	−1009 (20)	3510 (13)	−1869 (16)	H_2O (1)	4963 (31)	7146 (21)	−2952 (25)
O (10)	−2177 (23)	4375 (16)	−56 (19)	H_2O (2)	6264 (40)	5642 (27)	4072 (32)
C (5)	−2588 (30)	4294 (20)	−2328 (24)	H_2O (3)	1429 (39)	2280 (27)	−2983 (31)

Table 2. Atomic thermal parameters U_{ij} and their standard deviations (10^{-4} Å^2 units)
the temperature factor is defined as $\exp[-2\pi^2\sum_{ij}h_ih_ja_ia_jU_{ij}]$, $i, j=1,2,3$

Atom	U_{11}	U_{22}	U_{33}	$U_{12}/2$	$U_{13}/2$	$U_{23}/2$
Pt (1)	187 (5)	173 (5)	137 (5)	−132 (4)	84 (4)	−47 (4)
Pt (4)	291 (7)	314 (6)	163 (6)	−232 (6)	105 (5)	−44 (5)
Pt (2)	313 (5)	304 (4)	133 (4)	−244 (4)	114 (3)	−79 (3)
Pt (3)	287 (5)	265 (4)	175 (4)	−228 (4)	137 (4)	−109 (3)
Rb (1)	434 (16)	384 (14)	336 (14)	−241 (13)	168 (13)	−119 (12)
Rb (2)	534 (18)	605 (18)	345 (15)	−449 (16)	262 (14)	−174 (13)
Rb (3)	394 (14)	413 (14)	241 (12)	−265 (12)	151 (11)	−42 (10)
Rb (4)	928 (28)	851 (25)	343 (16)	−745 (24)	419 (18)	−331 (16)
Rb (5)	548 (19)	578 (19)	471 (18)	−417 (17)	292 (16)	−182 (15)

Isotropic vibration parameters of light atoms

O (1)	2.4 (0.3)	O (10)	2.5 (0.3)	C (9)	2.8 (0.5)
O (2)	2.2 (0.3)	C (5)	1.9 (0.4)	C (10)	1.7 (0.4)
C (1)	2.2 (0.4)	C (6)	2.1 (0.4)	O (19)	3.3 (0.4)
C (2)	2.0 (0.4)	O (11)	2.4 (0.3)	O (20)	2.8 (0.3)
O (3)	3.4 (0.4)	O (12)	3.0 (0.4)	O (21)	3.0 (0.4)
O (4)	3.0 (0.4)	O (13)	2.6 (0.3)	O (22)	2.4 (0.3)
O (5)	2.2 (0.3)	O (14)	2.6 (0.3)	C (11)	2.9 (0.5)
O (6)	2.6 (0.3)	C (7)	3.6 (0.6)	C (12)	2.5 (0.4)
C (3)	2.2 (0.4)	C (8)	4.0 (0.7)	O (23)	3.8 (0.4)
C (4)	1.8 (0.4)	O (15)	5.8 (0.6)	O (24)	4.3 (0.5)
O (7)	3.7 (0.4)	O (16)	6.7 (0.7)	H_2O(1)	4.4 (0.5)
O (8)	3.1 (0.4)	O (17)	1.9 (0.3)	H_2O(2)	6.5 (0.7)
O (9)	1.8 (0.3)	O (18)	1.8 (0.3)	H_2O(3)	6.3 (0.7)

Bulletin as Document No. 7936. All calculations were performed on a HITAC 8700/8800 computer at the Computer Center, University of Tokyo using a local version of UNICS.[9]

Chemical Analyses. The selected crystals were subjected to chemical analyses. The contents of the Rb atom and Pt atom were determined with the aid of atomic emission spectrometry and atomic absorption spectrophotometry. Nitric acid was added to increase solubility. For the atomic absorption spectrophotometer, a Nippon-Jarrell Ash FLA 100 equipped with an air-acetylene flame and a carbon rod furnace was used. Jarrell Ash AA-1 MK-II was used for by atomic emission spectrometry. Carbon and hydrogen were analyzed by the usual procedure, the results of which are given in Table 3. The stoichiometry indicated by the formula $Rb_{1.66}[Pt(C_2O_4)_2]\cdot 1.5H_2O$ has been obtained for RbDOX. There will be some uncertainty in the water content.

TABLE 3. CHEMICAL ANALYSES OF RbDOX

	Expected (%)	Found (%)
Rb	26.39	27.1
Pt	36.07	37.5
C	8.88	9.0
H	0.56	0.56

a) Ratio of Rb to Pt 1.66±0.07.

Electrical Conductivity Measurements. D.c. conductivity was measured using the four probe method. The measurements were made on several specimens along the needle axes parallel to the Pt chains of the crystals. The electrical

TABLE 4a. INTRAMOLECULAR BOND DISTANCES/Å

Pt(1)……O(1)	2.04(2)	O(13)……C(7)	1.36(5)
Pt(1)……O(2)	1.97(2)	O(14)……C(8)	1.34(4)
Pt(2)……O(13)	1.97(2)	C(7)……C(8)	1.46(4)
Pt(2)……O(14)	2.03(2)	C(7)……O(15)	1.25(4)
Pt(2)……O(17)	2.02(2)	C(8)……O(16)	1.27(5)
Pt(2)……O(18)	2.01(1)	O(17)……C(9)	1.43(3)
Pt(3)……O(5)	1.99(2)	O(18)……C(10)	1.29(4)
Pt(3)……O(6)	2.01(2)	C(9)……C(10)	1.49(5)
Pt(3)……O(9)	2.03(2)	C(9)……O(19)	1.21(5)
Pt(3)……O(10)	1.98(2)	C(10)……O(20)	1.21(3)
Pt(4)……O(21)	2.03(2)	O(21)……C(11)	1.36(6)
Pt(4)……O(22)	2.00(2)	O(22)……C(12)	1.30(4)
O(1)……C(1)	1.31(4)	C(11)……C(12)	1.51(4)
O(2)……C(2)	1.37(4)	C(11)……O(23)	1.25(4)
C(1)……C(2)	1.55(3)	C(12)……O(24)	1.25(6)
C(1)……O(3)	1.26(4)		
C(2)……O(4)	1.19(4)		
O(5)……C(3)	1.29(3)		
O(6)……C(4)	1.26(3)		
C(3)……C(4)	1.59(4)		
C(3)……O(7)	1.17(3)		
C(4)……O(8)	1.26(3)		
O(9)……C(5)	1.26(3)		
O(10)……C(6)	1.26(3)		
C(5)……C(6)	1.59(5)		
C(5)……O(11)	1.16(3)		
C(6)……O(12)	1.23(4)		

TABLE 4b. INTRAMOLECULAR BOND ANGLES/°

O(1)–Pt(1)–O(2)	84.3(8)	O(1)–C(1)–O(3)	123.4(2.2)
O(13)–Pt(2)–O(14)	85.7(8)	O(2)–C(2)–O(4)	120.8(2.3)
O(17)–Pt(2)–O(18)	85.4(7)	O(5)–C(3)–O(7)	129.2(2.8)
O(5)–Pt(3)–O(6)	81.4(8)	O(6)–C(4)–O(8)	124.6(2.6)
O(9)–Pt(3)–O(10)	80.8(8)	O(9)–C(5)–O(11)	124.4(2.8)
O(21)–Pt(4)–O(22)	84.6(9)	O(10)–C(6)–O(12)	127.9(3.2)
Pt(1)–O(1)–C(1)	110.7(1.6)	O(13)–C(7)–O(15)	117.7(3.0)
Pt(1)–O(2)–C(2)	114.6(1.6)	O(14)–C(8)–O(16)	116.8(3.1)
Pt(3)–O(5)–C(3)	116.8(1.7)	O(17)–C(9)–O(19)	115.8(3.0)
Pt(3)–O(6)–C(4)	114.8(1.9)	O(18)–C(10)–O(20)	124.2(2.8)
Pt(3)–O(9)–C(5)	115.3(1.7)	O(21)–C(11)–O(23)	117.9(3.4)
Pt(3)–O(10)–C(6)	116.0(1.8)	O(22)–C(12)–O(24)	123.3(2.9)
Pt(2)–O(13)–C(7)	109.7(2.1)	O(3)–C(1)–C(2)	118.0(2.6)
Pt(2)–O(14)–C(8)	107.1(2.0)	O(4)–C(2)–C(1)	127.4(2.6)
Pt(2)–O(17)–C(9)	107.3(1.5)	O(7)–C(3)–C(4)	119.1(2.5)
Pt(2)–O(18)–C(10)	112.6(1.6)	O(8)–C(4)–C(3)	119.6(2.6)
Pt(4)–O(21)–C(11)	107.7(2.3)	O(11)–C(5)–C(6)	122.4(2.9)
Pt(4)–O(22)–C(12)	112.3(1.7)	O(12)–C(6)–C(5)	117.7(2.4)
O(1)–C(1)–C(2)	118.3(2.3)	O(15)–C(7)–C(8)	126.0(3.5)
O(2)–C(2)–C(1)	111.8(2.3)	O(16)–C(8)–C(7)	125.2(3.2)
O(5)–C(3)–C(4)	111.4(2.4)	O(19)–C(9)–C(10)	127.5(2.6)
O(6)–C(4)–C(3)	115.5(2.2)	O(20)–C(10)–C(9)	118.6(2.8)
O(9)–C(5)–C(6)	112.7(2.2)	O(23)–C(11)–C(12)	122.9(3.2)
O(10)–C(6)–C(5)	114.4(2.8)	O(24)–C(12)–C(11)	120.9(2.9)
O(13)–C(7)–C(8)	116.3(2.6)		
O(14)–C(8)–C(7)	117.9(3.0)		
O(17)–C(9)–C(10)	116.6(3.0)		
O(18)–C(10)–C(9)	117.3(2.3)		
O(21)–C(11)–C(12)	117.9(2.7)		
O(22)–C(12)–C(11)	115.7(3.2)		

contacts were made by four 0.025 mm gold wires attached with aquadag. RbDOX behaves as a semiconductor from 305 K to 83 K. The room temperature conductivity is 7×10^{-3} $(\Omega\,cm)^{-1}$ and the activation energy is 0.077 eV.

Results and Discussion

The intramolecular distances of the $Pt(C_2O_4)_2$ complexes are given in Table 4a and the intramolecular angles are listed in Table 4b. The distorted nonlinear sixfold Pt atom chain is formed along the crystallographic b axis and involves six bis(oxalate) groups in one repeating unit of 17.11(1) Å. There are four nonequivalent Pt atoms. Pt(1) and Pt(4) lie at the centres of symmetry (0,0,0) and (0,1/2,0), while Pt(2) and Pt(3) lie at the general positions (0.0021, 0.1582, 0.0033) and (0.0172, 0.3166, 0.0132). The stacking of $Pt(C_2O_4)_2$ complexes is shown in Fig. 1.

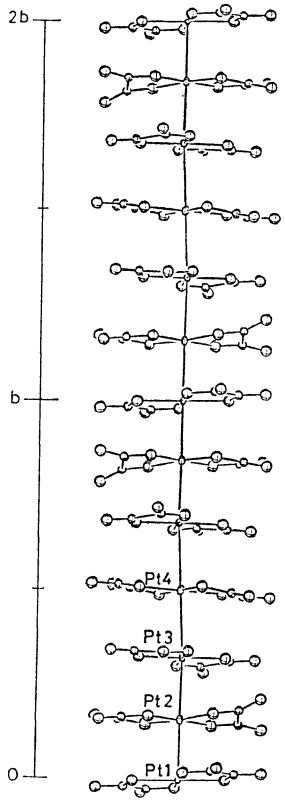

Fig. 1. The stacking of $Pt(C_2O_4)_2$ ions along the b axis. Two wavelengths of the Pt chain is shown.

The three independent Pt–Pt distances are Pt(1)–Pt(2)=2.717(3) Å, Pt(2)–Pt(3)=2.830(3) Å and Pt(3)–Pt(4)=3.015(3) Å. The Pt–Pt–Pt angles are Pt(1)–Pt(2)–Pt(3)=177.83(8)° and Pt(2)–Pt(3)–Pt(4)=174.23(5)°. The Pt–Pt distances in partially oxidized tetracyanoplatinate and bis(oxalato)platinate salts so far reported are shown in Table 5. The Pt–Pt distance of 2.717(3) Å found in RbDOX is the shortest spacing so far observed in partially oxidized platinate salts and shorter than the 2.77 Å interatomic separation in Pt metal itself. The Pt–O distances are 2.007(5) Å on average. Table 6 shows the averaged molecular structures of the four independent anions based on the assumption of D_{2h} symmetry. There appears to be a slight difference between the structure of the 3rd molecule and those of the others. Regarding the 3rd molecule, the O–Pt–O angle is 81.1(6)°, the C–O bond distance in the five membered ring is 1.27(2) Å and the C–C distance is on average 1.59(3) Å. This C–O bond is in the region of the C–O double bond. Regarding the other three molecules, the O–Pt–O angles are 85.0(4)° and the C–O distance is 1.35(1) Å. This bond length is close to that of the C–O single bond. The terminal C–O distances are in both cases 1.21(2) Å and 1.24(2) Å *i.e.*, those of normal double bonds. The structure of the third molecule is approximately equal to those of the molecules in $K_2[Pt(C_2O_4)_2]\cdot 2H_2O$,[20] $Co_{0.83}[Pt(C_2O_4)_2]\cdot 6H_2O$,[18] and $Mg_{0.82}[Pt(C_2O_4)_2]\cdot 5.3H_2O$.[17]

Figure 2 shows the mode of overlapping of platinate complex anions. The oxalate ligands are staggered with respect to the ligands directly above and below them along the chain. The staggered angles are approximately 46°, 55°, and 80°, while alternate ligands are eclipsed or staggered ≈90°. The 45° conformation has been found in the crystal of γ-KDOX. The 60° conformation has been observed in γ-KDOX and similar magnesium or cobalt defficient bis(oxalato)platinate complexes. It has been observed that these conforma-

Table 5. Comparison of the Pt–Pt distances in partially oxidized tetracyanoplatinate and bis(oxalato)platinate salts

	Crystal system	Pt–Pt distance/Å	Chain structure
$K_2[Pt(CN)_4]Br_{0.3}\cdot 3H_2O$[a]	tetragonal	2.888, 2.892	twofold structure
$Rb_2[Pt(CN)_4]Cl_{0.3}\cdot 3H_2O$[b]	tetragonal	2.877, 2.924	twofold structure
$(NH_4)_2[Pt(CN)_4]Cl_{0.3}\cdot 3H_2O$[c]	tetragonal	2.910, 2.930	twofold structure
$K_{1.75}[Pt(CN)_4]\cdot 1.5H_2O$[d]	triclinic	2.967, 2.976	fourfold structure
$K_2[Pt(CN)_4](FHF)_{0.3}\cdot 3H_2O$[e]	tetragonal	2.918, 2.928	twofold structure
$Rb_2[Pt(CN)_4](FHF)_{0.40}$[f]	tetragonal	2.798	twofold structure
$Cs_2[Pt(CN)_4](FHF)_{0.39}$[g]	tetragonal	2.833	twofold structure
$Mg_{0.82}[Pt(C_2O_4)_2]\cdot 5.3H_2O$[h]	orthorhombic	2.85	twofold structure
$Co_{0.83}[Pt(C_2O_4)_2]\cdot 6H_2O$[i]	orthorhombic	2.841	twofold structure
$K_{1.81}[Pt(C_2O_4)_2]\cdot 2H_2O$[j]	triclinic	2.961, 2.965	superstructure
$Cs_2[Pt(CN)_4](N_3)_{0.25}\cdot 0.5H_2O$[k]	tetragonal	2.877	twofold structure
$Rb_{1.67}[Pt(C_2O_4)_2]\cdot 1.5H_2O$[l]	triclinic	2.717, 2.830, 3.015	sixfold structure

a) Reference 10. b) Reference 11. c) Reference 12. d) Reference 13a, 13b. e) Reference 14. f) Reference 15. g) Reference 16. h) Reference 17. i) Reference 18. j) Reference 6. k) Reference 19. l) this work.

Table 6. The averaged molecular structures of the four independent Pt anions

	a/Å	b/Å	c/Å	d/Å	
I	2.00(1)	1.34(3)	1.55(3)	1.23(3)	
II	2.01(1)	1.36(2)	1.48(3)	1.24(2)	
III	2.00(1)	1.27(2)	1.59(3)	1.21(2)	
IV	2.02(2)	1.33(3)	1.51(4)	1.25(3)	
A	2.00	1.28	1.55	1.22	
B	2.013(5)	1.26(1)	1.57(2)	1.23(1)	
C	2.00	1.29	1.54	1.22	
	α/°	β/°	γ/°	δ/°	ε/°
I	84.3(8)	112.6(1.1)	115.1(1.6)	122.1(1.6)	122.7(1.8)
II	85.6(6)	109.2(9)	117.0(1.4)	118.6(1.5)	124.3(1.5)
III	81.1(6)	115.7(9)	113.5(1.2)	127.0(1.4)	119.7(1.3)
IV	84.6(9)	110.0(1.4)	116.8(2.1)	120.6(2.2)	121.9(2.2)
A	82	115	115	126	120
B	82.7(3)	113.1(4)	115.7(7)	124.5(7)	120.0(7)
C	83	113	116	124	120

A: $Mg_{0.82}[Pt(C_2O_4)_2]\cdot 5.3H_2O$; $Pt(C_2O_4)_2^{-1.64}$ B: $Co_{0.83}[Pt(C_2O_4)_2]\cdot 6H_2O$; $Pt(C_2O_4)_2^{-1.66}$ C: $K_2Pt(C_2O_4)_2\cdot 2H_2O$; $Pt(C_2O_4)_2^{-2}$.

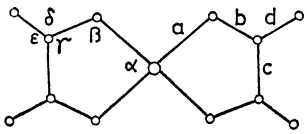

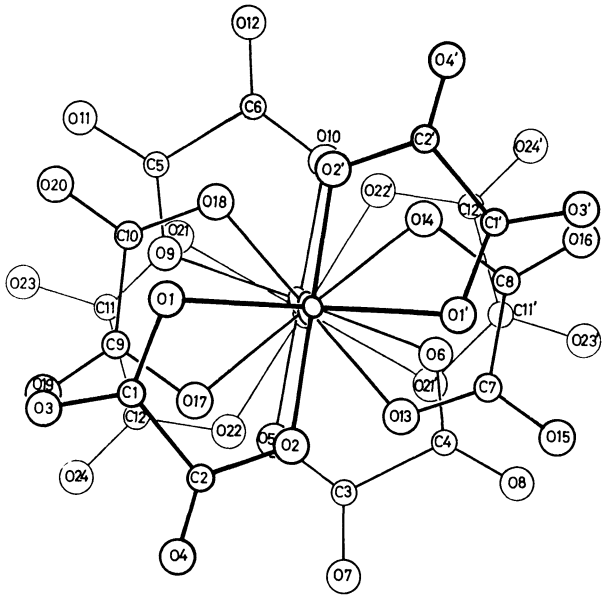

Fig. 2. The mode of overlapping of platinate complex anions.

tions are suitable for intermolecular stabilization due to the overlapping of the higher occupied molecular orbitals of one molecule and the lower unoccupied molecular orbitals of the neighbouring molecule. The importance of the charge transfer interactions in the stabilization of the molecular overlapping was first suggested in Miller's molecular back bonding theory.[21] The 80° conformation observed in this crystal is a new type conformation.

The equations of the best planes, perpendicular distances from these planes and the dihedral angles between these planes are listed in Tables 7a and 7b. The dihedral angles between the Pt(1), Pt(2), and Pt(3)

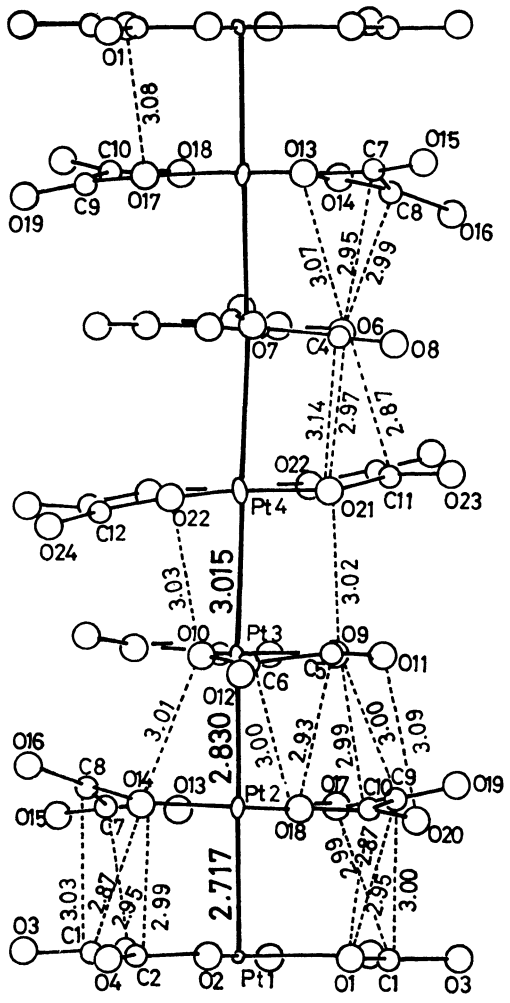

Fig. 3. Short intermolecular contacts (<3.1 Å) within the Pt chain.

Table 7a. Least-squares plane for the $Pt(C_2O_4)_2$ planes and deviations from the planes (X, Y and Z refer to the orthogonal coordinate system (Å) with X along a. Y is perpendicular to X in ab plane)

1) Pt(1) plane:
$-0.7152X+(-0.6980)Y+0.0355Z=0$

Atom	Deviation/Å
Pt(1)	0.0
O(1)	−0.07
O(2)	−0.04
C(1)	0.02
C(2)	0.01
O(3)	0.01
O(4)	−0.03

2) Pt(2) plane:
$-0.7414X+(-0.6707)Y+0.0232Z+2.8248=0$

Atom	Deviation/Å
Pt(2)	0.11
O(13)	0.13
O(14)	0.11
O(17)	−0.00
O(18)	0.14
C(7)	0.13
C(8)	−0.11
C(9)	−0.09
C(10)	0.12
O(15)	0.28
O(16)	−0.47
O(19)	−0.41
O(20)	0.28

3) Pt(3) plane:
$-0.7054X+(-0.7079)Y+0.0354Z+5.5226=0$

Atom	Deviation/Å
Pt(3)	−0.01
O(5)	0.06
O(6)	−0.02
O(9)	−0.06
O(10)	−0.02
C(3)	0.04
C(4)	−0.02
C(5)	−0.11
C(6)	0.04
O(7)	0.17
O(8)	−0.17
O(11)	−0.11
O(12)	0.22

4) Pt(4) plane:
$-0.6229X+(-0.7812)Y+(-0.0412)Z+8.4675=0$

Atom	Deviation/Å
Pt(4)	0.00
O(21)	0.07
O(22)	0.19
C(11)	−0.05
C(12)	0.03
O(23)	0.03
O(24)	−0.12

planes are 0.8—3.1°, but the Pt(4) plane is inclined to the other planes at 7.7—10.0°. Table 8 shows the short interatomic distances within the Pt chain and Figure 3 shows the short intermolecular contacts within the Pt chain.

Table 7b. Dihedral angles for the $Pt(C_2O_4)_2$ planes

		Dihedral angles/°
plane 1	plane 2	2.3
plane 1	plane 3	0.8
plane 1	plane 4	8.4
plane 2	plane 3	3.1
plane 2	plane 4	10.0
plane 3	plane 4	7.7

Table 8. Short interatomic distances/Å within the Pt chains (<3.1Å)

O(1)···C(10)	2.87(5)	O(6)···C(8)	2.99(8)
O(1)···C(9)	2.95(7)	O(6)···O(13)	3.07(4)
O(1)···C(7)	2.95(7)	O(9)···C(10)	3.00(5)
O(1)···O(17)	3.08(5)	O(9)···C(9)	3.00(5)
C(1)···O(14)	2.87(6)	O(9)···O(21)	3.02(5)
C(1)···O(17)	2.99(5)	O(9)···O(18)	3.04(5)
C(1)···C(9)	3.00(6)	O(10)···O(14)	3.01(5)
C(1)···C(8)	3.03(9)	O(10)···O(22)	3.03(5)
C(2)···O(17)	2.99(4)	C(5)···O(18)	2.93(5)
C(2)···O(14)	2.99(6)	C(5)···C(10)	3.01(5)
O(6)···C(11)	2.87(7)	C(6)···O(18)	3.00(4)
O(6)···C(7)	2.95(7)	O(11)···O(20)	3.09(4)
O(6)···O(21)	2.97(5)		
Pt(1)···Pt(2)	2.717(3)		
Pt(2)···Pt(3)	2.830(3)		
Pt(3)···Pt(4)	3.015(3)		

The Pt(1) plane is nearly planar but the Pt(2) plane is concave (Fig. 3). The Pt(2) atom is 0.11 Å shifted from the best plane toward the Pt(1) plane and the terminal oxygen atoms of the ligands O(16) and O(19) are 0.47 Å and 0.41 Å from the plane, respectively. The large deviation of these atoms from the plane is attributed mainly to the shortening of the Pt–Pt distance and partly to the interaction between the oxygen atoms of oxalate ligands and surrounding atoms. Figure 2 shows direct overlapping of the terminal oxygen atoms of the Pt(2) plane, O(16) and O(19), with O(3) and O(3′) atoms of the Pt(1) plane. The 46° staggered overlapping of the Pt(1) plane and the Pt(2) plane will be a very stable form considering the large intermolecular overlapping and the short interatomic distances within the chain. Many short interatomic contacts indicate that the charge transfer interactions between the ligands of the neighbouring molecules will have influence on the mode of overlapping. The Pt(3) plane is more planar than the Pt(2) plane but the terminal oxygen atoms of the ligands are shifted 0.11—0.22 Å from the plane. As to the Pt(4) plane, the oxygen atom in the five-membered ring shows a 0.19 Å deviation from the least-squares plane and the terminal oxygen atom is 0.12 Å distant from the plane. The Pt(4) plane has little overlapping with the molecules directly above and below. The inclination of the least-squares plane of the Pt(4) plane with respect to the other planes will be caused mainly by the longest Pt–Pt distance, small intermolecular overlapping and the interaction with Rb cations and the weak hydrogen bonding with water molecules. The short interatomic distances between

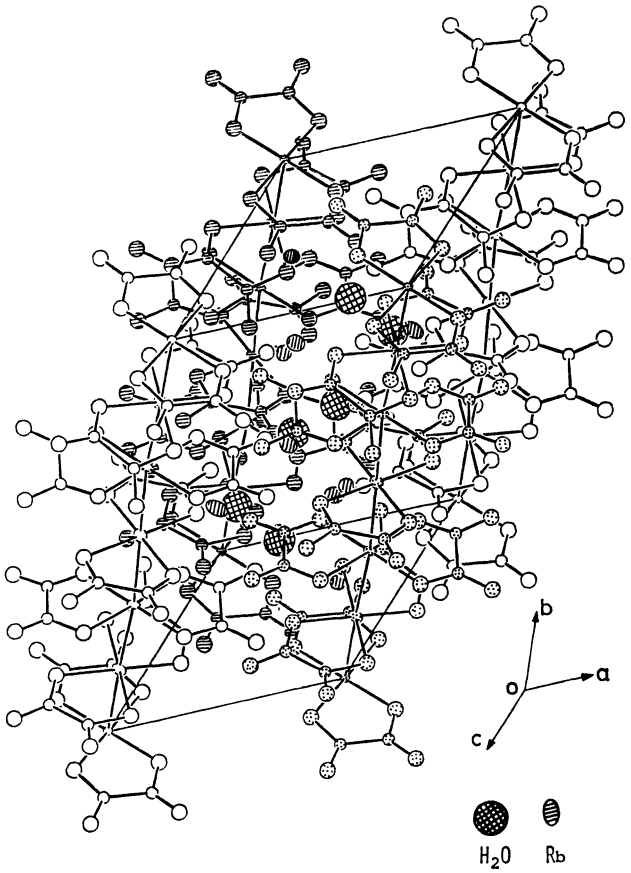

Fig. 4. Three-dimensional structure of RbDOX.

the terminal oxygen atoms of the Pt(4) plane and the Rb atoms or water molecules are as follows: O(23)···H_2O(2) 2.74 Å, O(23)···Rb(4) 3.01 Å and 3.09 Å, O(24)···Rb(4) 2.99 Å, O(24)···Rb(2) 2.89 Å. The crystal structure is shown in Fig. 4. The structure contains five independent Rb ions. Table 9 lists the interatomic distances within the coordination spheres to 3.3 Å around the Rb cations and the oxygen atoms of the water molecules. Rb(1), Rb(4) and Rb(5) are seven-coordinated ions, while Rb(2) and Rb(3) are eight-coordinated ones. Figures 5 and 6 show the c* axis and a* axis projections of the structure of RbDOX. The neighbouring Pt chains are not linked by hydrogen bonding of the water molecules but are linked by the coordinations of the terminal oxygen atoms to the Rb cations. The chain-chain interaction through Rb ions and water molecules do not appear to be so strong. Almost all the Rb^+···O distances exceed the Rb^+···O van der Waals sum (2.88 Å).

Peierls Distortion. A one-dimensional metallic system is unstable in the presence of changes in the crystal lattice period which split a partly filled band into completely filled and empty sub-bands. When the temperature is lowered, a one-dimensional metal should exhibit lattice distortions with a wave number equal to twice the Fermi momentum. The period of the Peierls distorted cell is determined by the degree of partial oxidation (DPO).[22]

Six Pt atoms and ten Rb atoms are found in the unit cell of RbDOX and the ratio of the content of Rb atoms to Pt atoms is 1.67, while the result of chemical analyses show that this ratio is 1.66. Thus the DPO of RbDOX is about 0.33. The possible period of the superlattice along the $Pt(C_2O_4)_2$ chain is $6nb_0(=2nb_0/\mathrm{DPO}; n=1,2,3\cdots)$, where b_0 is the average Pt–Pt distance. The case for $n=1$ ($\approx$17.1 Å) corresponds to the "$2k_F$-instability" of a one-dimensional metal. Thus the sixfold superstructure of RbDOX is confirmed as the structure of the commensurate Peierls state, produced by the condensation of $2k_F$ phonon, on the basis of the crystal structure determination, chemical analyses

Table 9. Short interatomic distances/Å within the coordination spheres to 3.3 Å around the Rb cations and oxygen atoms of water molecules

Rb(1)···$H_2O(1)^{a)}$	2.89(3)	Rb(5)···O(4)	3.00(3)
O(19)	2.90(2)	$H_2O(3)^{g)}$	3.06(4)
$O(8)^{g)}$	2.96(3)	$O(5)^{g)}$	3.08(3)
$O(20)^{i)}$	3.07(3)	$O(7)^{g)}$	3.17(3)
$O(15)^{e)}$	3.14(6)	O(13)	3.18(2)
$O(3)^{i)}$	3.16(2)	O(7)	3.21(4)
$O(7)^{g)}$	3.17(3)	O(17)	3.25(2)
Rb(2)···O(24)	2.89(5)	$H_2O(1)$···$O(4)^{e)}$	2.84(4)
$H_2O(2)^{j)}$	2.92(4)	$O(21)^{d)}$	2.86(4)
$O(12)^{d)}$	3.04(4)	$Rb(1)^{e)}$	2.89(3)
$O(10)^{b)}$	3.05(2)	$Rb(3)^{j)}$	3.07(5)
$O(4)^{g)}$	3.10(3)	$O(11)^{d)}$	3.29(4)
$O(18)^{d)}$	3.12(2)		
$O(12)^{b)}$	3.14(2)	$H_2O(2)$···$O(23)^{f)}$	2.74(5)
$O(2)^{g)}$	3.27(2)	$O(20)^{b)}$	2.90(4)
		$Rb(2)^{j)}$	2.92(4)
Rb(3)···$O(16)^{d)}$	2.86(6)	Rb(3)	3.23(5)
$O(12)^{b)}$	2.92(2)		
$O(20)^{f)}$	2.95(4)	$H_2O(3)$···O(9)	2.90(5)
$O(11)^{b)}$	2.98(2)	O(19)	2.91(7)
$O(11)^{f)}$	2.99(2)	$Rb(4)^{j)}$	3.00(6)
$O(3)^{g)}$	3.07(2)	$Rb(5)^{g)}$	3.06(4)
$H_2O(1)^{j)}$	3.07(5)	C(12)	3.24(7)
$H_2O(2)$	3.23(5)		
Rb(4)···$O(16)^{g)}$	2.95(5)		
$O(24)^{k)}$	2.99(3)		
$H_2O(3)^{k)}$	3.00(6)		
$O(23)^{l)}$	3.01(4)		
$O(8)^{g)}$	3.03(3)		
$O(23)^{k)}$	3.09(2)		
$O(6)^{g)}$	3.19(2)		

Symmetry code

a)	x,	$-1+y$,	z
b)	$-x$,	$1-y$,	$-z$
c)	x,	$1+y$,	z
d)	$1+x$,	y,	z
e)	x,	y,	$1+z$
f)	$1+x$,	y,	$1+z$
g)	$1-x$,	$-y$,	$-z$
h)	$1-x$,	$1-y$,	$1-z$
i)	$-x$,	$-y$,	$-1-z$
j)	$1-x$,	$1-y$,	$-z$
k)	$1-x$,	$-y$,	$-1-z$
l)	$1+x$,	$-1+y$,	z

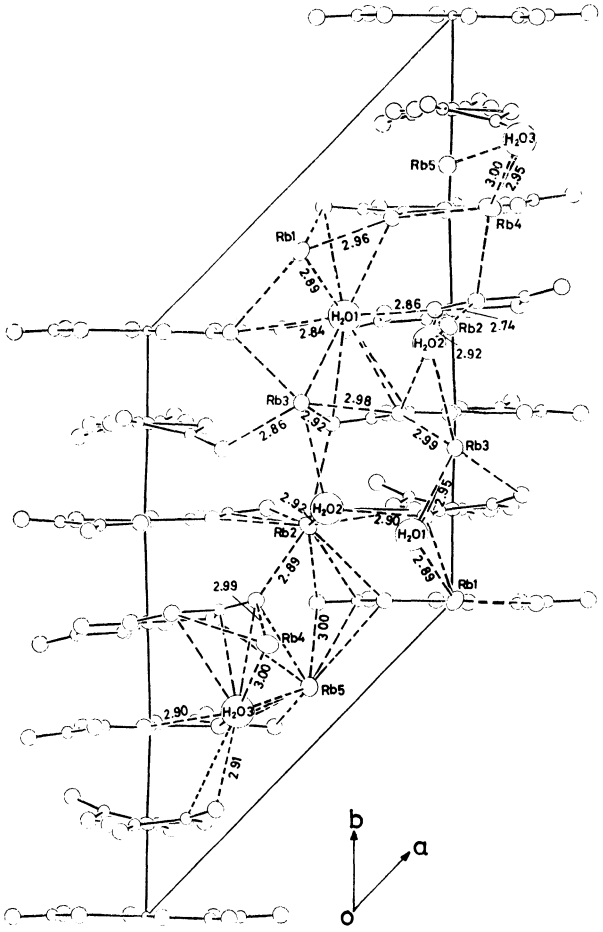

Fig. 5. The c* axis projection of the structure of RbDOX. Broken lines indicate some short interatomic contacts (<3.3 Å).

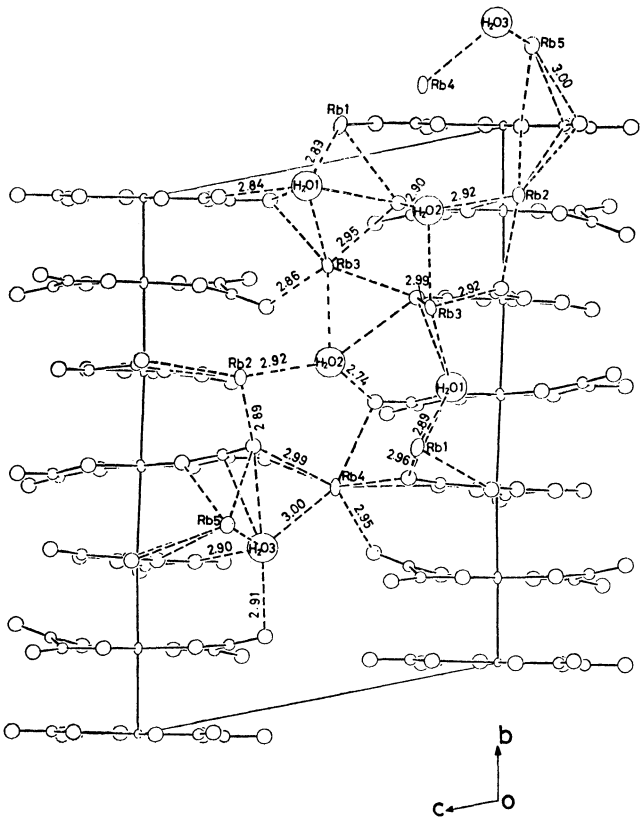

Fig. 6. The a* axis projection of the structure of RbDOX. Broken lines indicate some short interatomic contacts (<3.3 Å).

and the measurements of electrical conductivity. The longitudinal displacements of the Pt modulation wave from the point [(0.0, n/6, 0.0); n=0, ···5] are (0.0, 0.14, 0.16, 0.0, −0.16, −0.14 Å) respectively. These displacements can be approximately expressed in terms of the sinusoidal modulation wave. The amplitude of the modulation wave on the l-th platinum atomic position in the n-th cell [$n=(n_1,n_2,n_3)$] is given by $0.17\sin\{(2\pi/6)\text{-}(l-1)+n_2\}(l=1,\cdots 6)$. The transverse displacements of the Pt atoms are (0.0, 0.04, 0.16, 0.0, −0.16, −0.04 Å). It is logical that the transverse displacements can not be described as a simple sinusoidal wave, considering that the longitudinal displacements will be mainly influenced by interchain interactions whereas the transverse displacements will be also influenced by interchain interactions. Table 10 shows a comparison of the modulation waves in γ-KDOX, RbDOX, and KCP. The amplitudes of the modulation waves in RbDOX and γ-KDOX are approximately 0.17 Å, *i.e.* seven times as large as that of KCP. The correlation of the phase of the lattice modulation waves on the different chain is incomplete in KCP, while the superstructures of bis(oxalato)platinate complexes indicate complete correlation.

In the Peierls phase, the charge density along the platinum chain varies periodically with the wave number of $2k_F$. In order to gain the stabilization energy, Peierls gap is developed at the Fermi level to involve two holes in one repeating unit of the Pt chain. Besides the simple Peierls structure with wavelike charge

Table 10. Comparison of the structures of RbDOX, γ-KDOX,[a] and KCP[b]

	RbDOX	γ-KDOX	KCP(Br)
Chemical formula	$Rb_{1.67}[Pt(C_2O_4)_2]\cdot 1.5H_2O$	$K_{1.81}[Pt(C_2O_4)_2]\cdot 2H_2O$	$K_2[Pt(CN)_4]Br_{0.3}\cdot 3H_2O$
Crystal system	Triclinic	Triclinic	Tetragonal
Pt···Pt distance	2.72, 2.83, 3.02 Å,	2.84, 2.87 Å	2.89 Å
Modulation wave	Longitudinal (and transverse)	Transverse and longitudinal	Longitudinal
amplitude	0.17Å (at R.T.)	0.17 Å (at R.T.) (0.20, −0.08, 0.11) Å	0.025 Å (T<100 K)
period	$6\times R_{Pt\cdots Pt}$(17.1 Å)	$10.5\times R_{Pt\cdots Pt}$(30.0 Å)	$6.5\times R_{Pt\cdots Pt}$ (18.8 Å)
Orderness of the chain distortion	Complete (sixfold superstructure)	Complete (superstructure)	Incomplete (fluctuation of the lattice distortion)

a) Refs. 6 and 7. b) Ref. 3.

distribution, a sixfold superstructure of mixed valence configuration may be supposed,[23] that is, $6Rb_{1.67}[Pt(C_2O_4)_2]\cdot 1.5H_2O = (Rb^+)_{10}(Pt^{2+})_5(Pt^{4+})(C_2O_4^{2-})_{12}\cdot 9H_2O$. This model is consistent with the fact that the Pt atom is apt to be in the Pt^{2+} and Pt^{4+} ionic states, but the mixed valence model of the superstructure is opposed to the structural characteristics of platinate complexes: 1. This model is inconsistent with the appearance of a incommensurate superstructure like γ-KDOX. 2. Pt^{4+} has an octahedral configuration and Pt^{2+} has a square planar configuration. Owing to the difference in these coordination types, the distortion of the Pt chain will be localized around the Pt^{4+} site assuming "the mixed valence model" is valid.

The displacements of the Pt atoms in RbDOX or γ-KDOX are in fact described as sinusoidal waves. Based on this reasoning, the mixed valence model is not suitable for RbDOX and γ-KDOX.

Coulomb Interaction between Pt Chains with Charge Density Waves. The lattice distortion waves give rise to a periodical variation of the charge density along the Pt chains.[24] Since the charge density wave thus produced on the Pt chains interact with each other, the phase of the periodical distortion wave is considered to be governed by the interchain Coulomb coupling between the charge density waves. The superstructure formation accompanied by successive phase transitions between 54 K and 37 K in TTF-TCNQ and the development of the diffuse-scattering at $(\pi/a, \pi/a, 2k_F)$ in the KCP salt with lowering of temperature indicate that the chains are anti-phase ordered so as to minimize the Coulomb energy.[25] Figure 5 is the c* axis projection of the structure of RbDOX. The interchain distance is 8.75 Å which is the shortest in all the interchain distances. Assuming that charge density waves or some periodical charge distribution exists along the sixfold Pt chains, the phase difference between the neighbouring positions on these two chains must be about 180°. The wave length of CDW is considered to be equal to the periodicity of the Pt chain ($6\times r_{Pt\cdots Pt}$) and the phase difference between the lattice points must be $2\pi n (n=0,1,2,\cdots)$. Figure 5 seems to indicate that the nearest-neighbour chains tend to be anti-phase ordered. Figure 6 is the a* axis projection of the structure and the interchain spacing is 11.1 Å. The phase difference between the neighbouring positions on two Pt chains is about 50°.

Coulomb interaction between two chains with charge density waves $\rho_i=\rho_0\cos\Phi_i$ may be estimated by the following equation;[26]

$$U_{int} = (1/4\varepsilon_\perp)\rho_0^2[2K_0(2k_Fd)]\cos(\Phi_i-\Phi_j)$$
$$= (1/4\varepsilon_\perp)\rho_0^2\sqrt{\pi/2X}e^{-X}\cos(\Phi_i-\Phi_j) \quad X\gg 1$$

where $\varepsilon_\perp$ is the perpendicular static dielectric constant, $K_0(X)$ is the complete Elliptic Integral of the First Kind and d is the interchain spacing. Φ is the phase difference between the origin and the lattice point in the two dimensional lattice, the unit vectors of which are $\boldsymbol{a}_\perp$ and $\boldsymbol{c}_\perp$ which are perpendicular to the Pt chains (Fig. 7). Φ is expressed by the use of the phase parameters δ_a and δ_c, $\Phi_{n_1,n_2}=2\pi(\delta_a n_1+\delta_c n_2)$. The next examination was to establish whether the crystal lattice

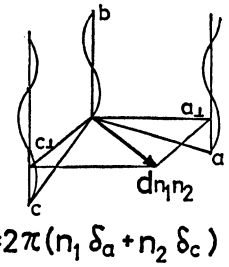

Fig. 7. The phase difference Φ between the platinum chains.

of RbDOX coincides with the structure which minimizes the Coulomb energy. The total Coulomb energy U_{tot} is proportional to

$$\sum_{n_1}\sum_{n_2}U(n_1,n_2) = \sum_{n_1}\sum_{n_2}\sqrt{1/X_{n_1,n_2}}e^{-X_{n_1,n_2}}\cos 2\pi\Phi_{n_1,n_2},$$
$$X_{n_1,n_2} = 2k_Fd_{n_1,n_2},$$

where $d_{n_1,n_2}(=|n_1\boldsymbol{a}_\perp+n_2\boldsymbol{c}_\perp|)$ is the interchain distance between the origin (0,0) and the lattice point (n_1,n_2). In this calculation, the lattice constants a, b, c and the angle between $\boldsymbol{a}_\perp$ and $\boldsymbol{c}_\perp$ are fixed. The result of the calculation for several values of δ_a and δ_c are shown in Fig. 8. The point where the total energy is a minimum

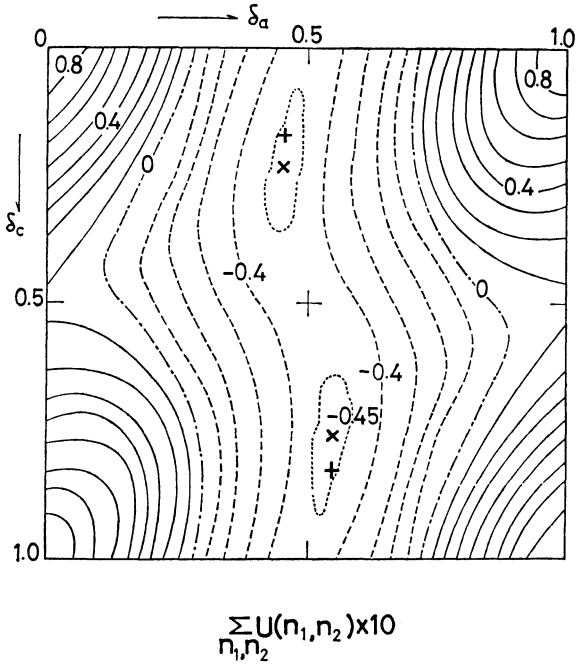

Fig. 8. Total Coulomb energies for various δ_a and δ_c. The point with the minimum total energy is indicated by a cross. Plus sign indicates the position of the parameters δ_a and δ_c derived from the lattice constants.

is indicated by a cross. A plus sign indicates the position of the parameters δ_a and δ_c derived from the lattice constants. The X-ray values of δ_a and δ_c can be calculated as (Fig. 9).

$$\delta_a = RA/OB = 0.537, \quad \delta_c = -R'C/OB = -0.138.$$

The agreement is satisfactory. A similar calculation

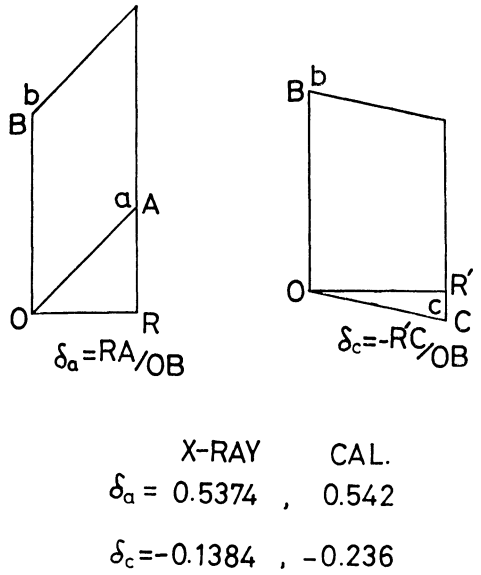

Fig. 9. The projection of the unit cell of RbDOX and the interchain phase differences δ_a and δ_c.

was made for γ-KDOX. The lattice of γ-KDOX is modulated by incommensurate distortion wave. The lattice constants of the fourfold fundamental structure of γ-KDOX are $a=9.749(9)$, $b=11.403(18)$, $c=10.694(8)$ Å, $\alpha=99.54(9)$, $\beta=115.81(9)$, $\gamma=102.32(17)°$. The modulation wave is described by $\boldsymbol{P}\sin(\boldsymbol{K}\cdot\boldsymbol{R})$, where $\boldsymbol{P}$ and $\boldsymbol{K}[=(2\pi\phi_1, 2\pi\phi_2, 2\pi\phi_3)]$ are the amplitude and the wave vector, respectively. The components of $\boldsymbol{K}/2$ along the reciprocal axes a*, b*, and c* are $\phi_1=0.30$, $\phi_2=-0.38$ and $\phi_3=0.05$. X-Ray values of δ_a and δ_c have two terms. $\delta_a=RA/OB+\phi_1=0.403$, $\delta_c=RC/OB+\phi_3=0.250$, ϕ_1 and ϕ_3 are the contributions from the sinusoidal modulation wave. The calculated values of δ_a, δ_c are $\delta_a=0.482$, $\delta_c=0.206$. Good agreement was again obtained. The calculations show that γ-KDOX and RbDOX have crystal lattices in which the interchain Coulomb energies are minimum. The total energy is almost independent of δ_c around the position of the energy minimum which indicates the strong tendency of the anti-phase ordering of the nearest-neighbour chains.

References

1) R. Comès, M. Lambert, H. Launois, and H. R. Zeller, *Phys. Rev. B*, **8**, 571 (1973).
2) C. F. Eagan, S. A. Werner, and R. B. Saillant, *Phys. Rev. B*, **12**, 2036 (1975).
3) J. W. Lynn, M. Iizumi, and G. Shirane, *Phys. Rev. B*, **12**, 1154 (1975).
4) "Chemistry and Physics of One-Dimensional Metals," ed by H. J. Keller, Plenum Press, New York and London (1977).
5) A. J. Heeger and A. F. Garito, "Low Dimensional Cooperative Phenomena," ed by H. J. Keller, Plenum Press, New York (1975).
6) H. Kobayashi, I. Shirotani, A. Kobayashi, and Y. Sasaki, *Solid State Commun.*, **23**, 409 (1977).
7) A. Kobayashi, Y. Sasaki, I. Shirotani, and H. Kobayashi, *Solid State Commun.*, **26**, 653 (1978).
8) "International Tables for X-Ray Crystallography," Kynoch Press, Birmingham (1974), Vol. VI.
9) The Universal Crystallographic Computation Program System, Crystallographic Society of Japan (1967).
10) G. Heeger, H. J. Deiseroth, and H. Schulz, *Acta Crystallogr., Sect. B*, **34**, 725 (1978).
11) J. M. Williams, P. L. Johnson, A. J. Schultz, and C. C. Coffey, *Inorg. Chem.*, **17**, 834 (1978).
12) P. L. Johnson, A. J. Schultz, A. E. Underhill, D. M. Watkins, D. J. Wood, and J. M. Williams, *Inorg. Chem.*, **17**, 839 (1978).
13) a) J. M. Williams, K. D. Keefer, D. M. Washecheck, and N. P. Enright, *Inorg. Chem.*, **15**, 2446 (1976); b) A. H. Reis, Jr., S. W. Peterson, D. M. Washecheck, and J. S. Miller, *Inorg. Chem.*, **15**, 2455 (1976).
14) R. K. Brown, P. L. Johnson, T. J. Lynch, and J. M. Williams, *Acta Crystallogr., Sect. B*, **34**, 1965 (1978).
15) A. J. Schultz, C. C. Coffey, G. C. Lee, and J. M. Williams, *Inorg. Chem.*, **16**, 2129 (1977).
16) A. J. Schultz, D. P. Gerrity, and J. M. Williams, *Acta Crystallogr., Sect. B*, **34**, 1673 (1978).
17) K. Krogmann, *Z. Anorg. Allg. Chem.*, **358**, 97 (1968).
18) A. J. Schultz, A. E. Underhill, and J. M. Williams, *Inorg. Chem.*, **17**, 1313 (1978).
19) R. K. Brown, D. A. Vidusek, and J. M. Williams, *Inorg. Chem.*, **18**, 801 (1979).
20) R. Mattes, and K. Krogmann, *Z. Anorg. Allg. Chem.*, **332**, 247 (1964).
21) J. S. Miller, *Inorg. Chem.*, **15**, 2357 (1976).
22) K. Krogmann, "One-Dimensional Conductors," ed by J. Ehlers, K. Hepp, and H. A. Weidenmüller (Springer-Verlag, 1975).
23) H. Nagasawa, *J. Phys. Soc. Jpn.*, **45**, 701 (1978).
24) M. J. Rice, "Low-Dimensional Cooperative Phenomena," ed by H. J. Keller, Plenum Press, New York (1975).
25) J. Friedel, "Electron-Phonon Interactions and Phase Transitions," ed by T. Riste, Plenum Press, New York (1977).
26) a) A. J. Heeger, "Chemistry and Physics of One-Dimensional Metals," ed by H. J. Keller, Plenum Press, New York (1977); b) K. Saub, S. Barisic, and J. Friedel, *Phys. Lett. A.*, **56**, 302 (1976).